Eur. Phys. J. D **12**, 415–423 (2000)

THE EUROPEAN PHYSICAL JOURNAL D

EDP Sciences

Reflection of thermal atoms by a pulsed standing wave

P. Ryytty[a] and M. Kaivola

Department of Engineering Physics and Mathematics, Helsinki University of Technology, 02015 HUT, Finland

Received 3 December 1999 and Received in final form 25 April 2000

Abstract. Reflection of thermal atoms by a pulsed standing wave with a duration in the nanosecond range is studied. The momentum distribution of the reflected atoms is determined by calculations based on the adiabatic atom-photon interactions. It is shown that with a proper choice of the field intensity and the pulse duration the standing-wave pattern functions as a row of independent atom mirrors. At an optimum choice of the parameter values, the fraction of the elastically reflected atoms is more than 20%. Furthermore, we show that the pulsed standing-wave mirror can be used to manipulate their final momentum distribution. When using laser pulses with an intensity of several tens of MW/cm^2, tens of thousands of atoms can be reflected by a single laser pulse.

PACS. 32.80.Lg Mechanical effects of light on atoms, molecules, and ions

1 Introduction

The use of light forces in reflecting neutral atoms has been studied intensively during the past decade [1–3]. It has been shown both theoretically and experimentally that in a near-resonant interaction, coherent reflection of neutral atoms can be achieved by using the dipole forces exerted on the atoms in an inhomogeneous optical field. This has lead to the invention of several types of atom mirrors, including the evanescent-wave mirror formed in total internal reflection of light on a vacuum-dielectric interface [4–6] as well as various types of mirrors based on focused light fields such as the doughnut-mode optical field [7]. More recently, it has also been proposed that a standing wave could be used as a periodic reflector for matter waves in analogy to the dielectric multi-layer mirrors used in classical optics [8–10]. Atom mirrors that are based on light forces are presently widely used in various application of atom optics, *e.g.*, in confining neutral atoms into gravitational cavities [7,11], as atomic wave guides [12,13] or as mirrors in atom interferometers [14,15].

Commonly, atom mirrors are realized using continuous-wave (CW) lasers as the light source. Due to the relatively low field intensities available from the wavelength-tunable CW lasers the reflectivity of conventional atom mirrors rapidly decreases for atomic velocities on the order of a meter per second or higher. This velocity limit may be increased somewhat by applying field enhancement techniques such as the surface plasmon effect or optical build-up cavities [16–19]. These techniques are, however, far too ineffective for the reflection of atoms with velocities in the thermal range. The use of the conventional atom mirrors is then limited to grazing incidence reflection of atomic beams or to the control of initially laser cooled atoms. Furthermore, since the magnitude of the light forces at low field intensities is very sensitive to the internal energy-level structure of the atom, the conventional atom mirrors are suitable for the reflection of some particular atomic species only.

In this work, we study the use of a pulsed standing wave with a duration in the nanosecond range for the reflection of thermal atoms. When using a pulsed laser as the light source, the field intensity can be increased by several orders of magnitude as compared to the case of a typical CW laser. Due to the increased field strength the dipole forces become strong enough to significantly affect the atomic motion up to velocities of several tens of meters per second. This allows large angle reflection of atomic beams or even reflection of thermal atoms at normal incidence. Also, in the case of pulsed fields the dipole forces experienced by the particles remain strong even at large detunings from the atomic resonance. Pulsed atom mirrors will not, therefore, be sensitive to the internal energy-level structure of the atom. Consequently, atom optical components based on pulsed laser fields are useful also for the manipulation of multilevel atoms and even molecules [20–23].

The use of pulsed standing waves in deflecting atomic beams has been studied previously by various research groups [24–27]. In these works, the atoms move at right angles to the laser beams and, consequently, only spreading of the atomic beam in the transverse direction is observed. In contrast, we assume here that the atoms move nearly, parallel to the laser beams and study the effects of the pulsed standing wave on the velocity distribution of the atomic beam. We show that with a suitable choice of the field intensity and pulse duration each period

[a] e-mail: pryytty@cc.hut.fi

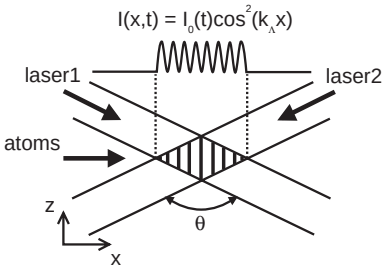

Fig. 1. The standing-wave geometry used for studying the atomic reflection.

of the standing-wave pattern acts as an elastic reflector for the incoming atoms. As a potential application for such a row of atom mirrors we consider reflection of thermal atoms at normal incidence.

We start by introducing the theoretical model that is used for the simulation of the atomic motion in the light field. The forces exerted on the atoms are modeled by an effective potential due to the adiabatic atom-photon interactions. The calculations are done in the quasiclassical approximation that neglects $\hbar k$-scale features in the atomic distributions. This is realistic, since the total momentum transferred to the atoms in a pulsed laser field is typically much larger than a single recoil momentum. The resulting equations of motion for the atomic center of mass are then used to determine the atomic momentum distribution after interaction with a single laser pulse.

2 Atomic motion in a pulsed standing wave

In this section, we study the motion of a beam of two-level atoms in a pulsed standing wave with a duration of several nanoseconds. The standing wave is formed in the overlap region of two counter-propagating laser beams, as shown in Figure 1. The wave fronts of the cosine squared intensity distribution are normal to the atomic beam, which is directed along the x-axis. The period Λ of the standing-wave pattern depends both on the wavelength λ of the light field and on the angle θ between the laser beams according to the relation $\Lambda = \lambda/[2\sin(\theta/2)]$. The transverse profile of the beams is taken to be square-shaped and their intensity to be in a range of tens to hundreds of MW/cm^2.

For coherent atom-photon interaction, the motion of the atoms in the laser field can conveniently be described by the dressed-atom approach [28,29]. In this approach, the atom and the laser field are considered to form a combined system and the resulting eigenstates of the total Hamiltonian, the dressed states, are used to determine the effects of the laser field on the atomic motion. In an uncoupled basis, the eigenstates are bunched into manifolds of two states with an energy separation of $\hbar\Delta$ within each manifold, where Δ is the detuning from the atomic resonance. When the atom-photon interaction is taken into account, the energy separation becomes intensity dependent. The energy shifts of the two dressed states within each manifold are then

$$U(x,t) = \pm\frac{1}{2}\hbar\sqrt{\Delta^2 + \Omega(x,t)^2}. \tag{1}$$

The Rabi frequency is defined as $\Omega(x,t) = \mu E(x,t)/\hbar$, where μ is the dipole matrix element for the transition and $E(x,t)$ is the amplitude of the electromagnetic field. If transitions between the different dressed states can be neglected, the energy shift $U(x,t)$ can be regarded as an effective potential seen by the atomic center of mass [28]. Atoms moving in a standing wave will thus experience a position dependent potential that in the case of a large detuning is sinusoidal. The center-of-mass motion of the atoms can then be determined by solving the scalar Schrödinger equation with the effective potential describing the light forces. This model for the atomic motion is valid, if $\Delta \gtrsim \Omega$ and if the laser field changes smoothly in time, *i.e.*, $\Delta \gg 1/\delta t$, where δt is the turn-on time of the laser pulse [28,30]. In our calculations, we use a detuning of $\Delta = 5\Omega_0$, where Ω_0 is the Rabi frequency corresponding to the amplitude of the standing wave at the peak of the laser pulse. For the laser intensities considered here, Ω_0 is on the order of 10^{12} s^{-1}. Since this is much larger than both $1/\delta t$ for a smooth laser pulse of nanoseconds duration and the Doppler shift caused by the atomic motion at velocities considered here, we can safely neglect the nonadiabatic effects in our calculations.

To determine the atomic momentum distribution after interaction with the pulsed standing wave it is convenient to use the Wigner function representation for the atomic center of mass [31]. In the case of a pulsed laser field, the induced atomic momentum will be large as compared with the single recoil momentum $\hbar k$. The calculation of the atomic Wigner function $f(x,p,t)$ can therefore be done in the quasiclassical approximation, which neglects $\hbar k$-scale features in the atomic distributions [32–34]. In this approximation, the equation of motion for the Wigner function simplifies to the classical Liouville equation

$$\left(\frac{\partial}{\partial t} + \frac{p}{m}\frac{\partial}{\partial x}\right) f(x,p,t) = \frac{\partial U(x,t)}{\partial x}\frac{\partial}{\partial p} f(x,p,t), \tag{2}$$

where m is the mass of the atom and p is the center-of-mass momentum. The momentum distribution of the atoms after interaction with the light field can now be found by solving the Wigner function for an appropriate initial distribution and by integrating it over the position space.

Equation (2) describes the motion of an atom in a classical potential. Therefore, an alternative method to calculate the final momentum distribution is to use the classical equations of motion with the gradient of the effective potential representing the light forces. For the pulsed standing wave the equations can be written as

$$\begin{aligned} \frac{\mathrm{d}\xi}{\mathrm{d}\tau} &= 4q \\ \frac{\mathrm{d}q}{\mathrm{d}\tau} &= -\frac{\Omega_0^2(\tau)}{4\epsilon}\frac{\sin(\xi)}{\left[\Delta^2 + \Omega^2(1+\cos(\xi))/2\right]^{1/2}}. \end{aligned} \tag{3}$$

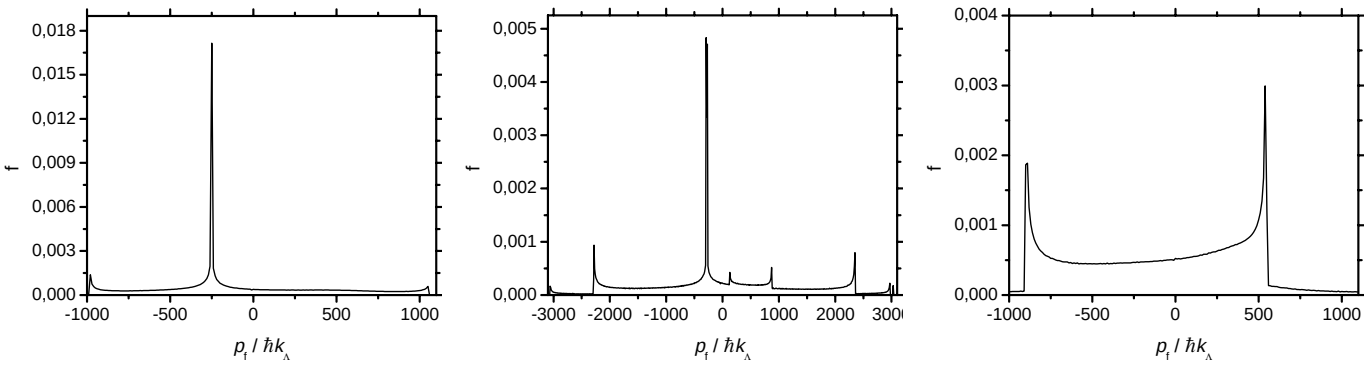

Fig. 2. The final momentum distribution of a beam of sodium atoms with an initial momentum of $250\,\hbar k_\Lambda$ after interaction with a pulsed standing wave. The distributions are calculated for a laser pulse with a fast turn on/off and 10 ns duration. The initial atomic distribution is chosen to be spatially evenly distributed over the interaction region formed by a single period of the standing-wave pattern. For (a) $\Omega_0 = 3.4 \times 10^{12}$ s^{-1}, $\Delta = 1.7 \times 10^{13}$ s^{-1} ($T_{\rm osc} = 19$ ns), (b) $\Omega_0 = 2.95 \times 10^{13}$ s^{-1}, $\Delta = 1.5 \times 10^{14}$ s^{-1} ($T_{\rm osc} = 6.5$ ns), and (c) $\Omega_0 = 7 \times 10^{12}$ s^{-1}, $\Delta = 3.5 \times 10^{13}$ s^{-1} ($T_{\rm osc} = 13$ ns). The wavelength of the light field is 589 nm and the angle between the laser beams is 180 degrees, in all cases. The vertical axis gives the fraction of atoms that end up in a final momentum state $m\hbar k_\Lambda$, where m is an integer.

Here we have used dimensionless units

$$\tau = \epsilon t, \quad q = p/(\hbar k_\Lambda), \quad \xi = 2k_\Lambda x, \tag{4}$$

where $\epsilon = \hbar k_\Lambda^2/(2m)$ is the recoil energy in units of angular frequency and k_Λ is the wave number of the standing wave. The final momentum distribution can now be calculated by using equations (3) to propagate the initial distribution of the atoms over the interaction time T. In the following calculations we use this method to determine the final momentum distributions. We assume that the atoms are initially evenly distributed in the position space. This allows us to limit the calculation to a single period of the effective potential. The occupation of a particular final momentum state is determined by counting the total number of atoms with a momentum corresponding to that state at the end of the laser pulse.

We start the analysis of the pulsed standing-wave mirror by applying harmonic approximation to the effective potential, *i.e.*, $U = m\omega_{\rm osc}^2 x^2/2$. In this case, atoms will go into an oscillatory motion around $x = 0$ with a period of oscillation of $T_{\rm osc} = 2\pi/\omega_{\rm osc}$. For laser pulses with a square-shaped temporal profile the oscillation period will be constant. By using harmonic analysis it is then easy to see that for interaction times satisfying

$$T = \left(n - \frac{1}{2}\right) T_{\rm osc} \quad (n = 1, 2, ...), \tag{5}$$

all the atoms will end up having a final momentum of $p_{\rm f} = -p_{\rm i}$, regardless of their velocity and x-coordinate value at the onset of the laser pulse [35]. With this choice of the interaction time the harmonic potential acts as an elastic reflector for the atoms. For red detuning the effective potential formed by a standing wave is nearly harmonic in the regions around the antinodes. These regions can, therefore, be utilized to elastically reflect the incoming atoms by choosing the interaction time and the oscillation period according to the relation (5). For a standing wave the oscillation frequency can be written to the lowest order as

$$\omega_{\rm osc} = k_\Lambda v_{\rm max}, \tag{6}$$

where $v_{\rm max} = (2\delta U/m)^{-1/2}$ and δU is the depth of the effective potential. The above relation shows that the oscillation period can be varied by changing the intensity or the angle between the laser beams. Therefore, with a suitable choice of the parameter values the standing wave can be made to act as a long row of independent atom mirrors. Of course, since the depth of the effective potential is limited, the pulsed standing-wave mirror can be efficiently used only for atoms with an initial velocity $v_{\rm i} < v_{\rm max}$. At higher initial velocities the standing wave will not have a significant influence on the atomic motion.

In Figure 2, we show the final momentum distribution of a monoenergetic beam of sodium atoms after interaction with a pulsed standing wave of 10 ns duration. The atomic motion during the laser pulse was calculated by solving equations (3) numerically. For the sake of clarity, the calculations were done assuming laser pulses with a fast turn on and off, *i.e.*, $I_0(t) = I_0$ when $0 \le t \le T$ and $I_0(t) = 0$ otherwise, where $I_0(t)$ is the intensity modulation of the standing-wave pattern. In all cases, the initial momentum of the atoms was taken to be $250\,\hbar k_\Lambda$. In Figure 2a the oscillation period was chosen to be such that $T_{\rm osc} \approx 2T$ ($n = 1$). Clearly, with this choice a significant fraction of the atoms are reflected nearly elastically. Roughly 20 % of the atoms occupy the states around the momentum of $-250\,\hbar k_\Lambda \pm 2\sigma$, where $\sigma = 10\hbar k_\Lambda$ is the FWHM of the peak. The spreading of the atoms to other momentum states is caused by the anharmonicity of the effective potential. The anharmonicity effects also start to diminish

the fraction of the elastically reflected atoms for initial velocities of $v_\mathrm{i} \gtrsim \Lambda/2T$. These effects will become more pronounced at higher intensities at which the atoms undergo several oscillations in the potential well during the laser pulse. In Figure 2b, for example, the oscillation period is $T_\mathrm{osc} \approx 2T/3$ ($n = 2$). The final momentum distribution is still peaked at the momentum of $-250\,\hbar k_\Lambda$, but the fraction of the atoms around this momentum is diminished to 10%. To increase the fraction of the elastically reflected atoms, the effective potential should be modified such that the quadratic part around the antinodes (nodes) covers a wider region of each period of the standing-wave pattern. In the case of simple atoms, this can be done for example with the aid of a bichromatic standing wave that in some cases can produce a nearly quadratic potential over the whole period [36].

In Figure 2c the oscillation period is chosen not to satisfy condition (5) for the optimum performance of the mirror. In this case, the atoms will spread to a wide range of momentum states thus significantly reducing the fraction of the elastically reflected atoms. However, the occupation of the negative momentum states can still be reasonably high compared with that of the positive momentum states. We conclude that for such a non-optimum choice of the oscillation period, the pulsed standing wave can function as an *inelastic* reflector for atoms. In the next section, we show how this kind of an inelastic reflector can be applied, for example, to reflect thermal atoms and to modify their final momentum distribution.

The above results show that a standing wave formed by a laser pulse with a fast turn on and off can be used as a row of independent atom mirrors. For a more realistic pulse shape such as, *e.g.*, a laser beam with a Gaussian temporal profile the final momentum distributions will be somewhat different as compared with the previous results. At low intensities ($T_\mathrm{osc} \gtrsim 2T$) the temporal profile of the laser pulse does not have a significant influence on the characteristics of the pulsed standing-wave mirror. With a suitable choice of the field intensity and pulse duration, a similar final momentum distribution as shown, *e.g.*, in Figure 2a can be obtained. The main difference is that the optimum for elastic reflection occurs at a slightly higher peak intensity of the laser field than was found in the case of a square-type temporal profile of the laser pulse. This is due to the fact that the maximum momentum that can be transferred to the atoms increases more slowly as a function of the field intensity for a smooth pulse profile than is the case for the fast turn on of the field [34].

For higher laser intensities ($T_\mathrm{osc} < T$) the atomic dynamics in the standing wave depends more on the temporal profile of the laser pulse. However, for atoms with initial velocities of $v_\mathrm{i} \lesssim \Lambda/2T$ the final momentum distributions are still not significantly changed when using a smooth laser pulse. At higher initial velocities the anharmonicity of the effective potential starts to dominate the atomic motion. In this case, the profile of the laser pulse can greatly influence the shape of the final momentum distributions. For example, in the case of a square-type pulse profile the maximum initial velocity that can be reflected is highest for initial x-coordinate values close to the antinodes of the standing wave (red detuning). When moving closer to the node positions, the height of the potential barrier decreases and, consequently, the maximum reflected velocity also decreases. Thus, a standing wave with a square-type pulse profile is most effective for the reflection of atoms that start close to the antinodes. This is not, however, the case when using a laser pulse with a smooth temporal profile. In this case, fast atoms that are located close to a node position can move to a neighboring period of the standing-wave pattern during the start of the laser pulse. These atoms can then be reflected by the neighboring atom mirror when the field intensity has reached a level high enough to significantly affect their motion. For example, in Figure 3 we show some typical trajectories for atoms moving in a standing wave formed by a laser pulse with a square or a Gaussian temporal profile. The temporal e^{-2} width of the Gaussian pulse and the duration of the square pulse are both 10 ns. The curves represent atomic trajectories for different initial velocities. In conclusion, the standing wave with a smooth pulse profile reflects most efficiently atoms in certain initial velocity groups in contrast to the case of a square profile laser pulse, which is most efficient for atoms that start at close to the antinodes [37]. Since the atomic motion at initial velocities of $v_\mathrm{i} \gtrsim \Lambda/2T$ is anharmonic, the fraction of the elastically reflected atoms will in general be rather small. To optimize the elastic reflection the period of the standing-wave pattern should be increased such that $T_\mathrm{osc} \approx 2T$.

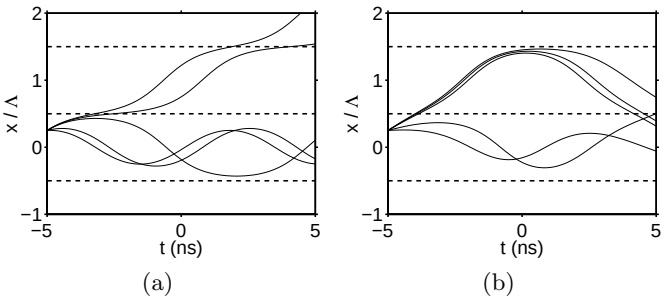

Fig. 3. The differences in atomic motion in a pulsed standing wave with two types of temporal profiles; (a) corresponds to a laser pulse with a fast turn on/off and (b) to a laser pulse with a Gaussian temporal profile. The curves represent atomic trajectories for different initial velocities. The e^{-2} width of the Gaussian profile and the length of the square-type laser pulse are both 10 ns. The pulse areas are equal in both cases.

In the previous paragraphs we showed how a pulsed standing wave can be used to reflect atoms with initial kinetic energy lower than the depth of the effective potential. At higher initial velocities, the maximum momentum that can be transferred to the atoms will be inversely proportional to the initial velocity. Therefore, only a small fraction of the potential energy of the standing wave can be transferred to kinetic energy of the fast atoms. However, this situation can be changed by making the standing-wave pattern move during the laser pulse.

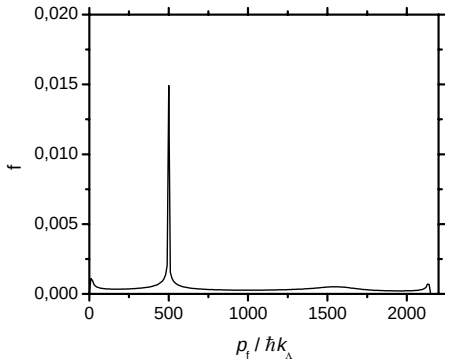

Fig. 4. The final momentum distribution of a beam of sodium atoms with an initial momentum of $1500\,\hbar k_\Lambda$ after interaction with a standing-wave pattern moving with a velocity of 30 m/s. The distribution is calculated for a laser pulse with a fast turn on/off and 10 ns duration. The initial atomic distribution is chosen to be evenly distributed over the interaction region. The laser intensity was chosen to give $T_{\rm osc} \approx 2T$. The period of the standing-wave pattern is $\Lambda = 294.5\,\rm nm$.

This kind of a moving standing wave can be formed, for example, by creating a small frequency difference ω_δ for the two counter-propagating laser beams. In this case, the intensity distribution of the standing-wave pattern has the form

$$I(\xi,\tau) = \frac{1}{2} I_0(\tau)\left[1 - \cos(\xi - \omega_\delta \tau/\epsilon)\right], \qquad (7)$$

i.e., the standing-wave pattern moves with a velocity of $v_{\rm sw} = \omega_\delta / 2k_\Lambda$. If the calculations are done in a coordinate frame that moves with this velocity, it is easy to see that the atomic motion can be determined by solving equations (3) with initial values $\tilde{q}_{\rm i} = q_{\rm i} - m v_{\rm sw}/\hbar k_\Lambda$. Therefore, atoms with an initial velocity in the range of

$$v_{\rm sw} - v_{\rm max} \le v_{\rm i} \le v_{\rm sw} + v_{\rm max} \qquad (8)$$

experience the effects of the moving standing-wave pattern just as atoms with $v_{\rm i} \le v_{\rm max}$ in the case of a stationary wave pattern. Now, however, the reflection takes place with respect to the momentum state $q = m v_{\rm sw}/\hbar k_\Lambda$ instead of the $q = 0$ state. In this case, the energy that can be transferred to the atoms approaches in magnitude the depth of the modulation of the effective potential regardless of the initial velocity. This offers a possibility to use the standing-wave mirror to efficiently manipulate atomic motion at higher initial atomic velocities. As an example, in Figure 4 we show the final momentum distribution of an atomic beam with an initial momentum of $1500\hbar k_\Lambda$ after interaction with a standing wave moving with a velocity of 30 m/s ($m v_{\rm sw} \approx 1000\hbar k_\Lambda$). The distribution was calculated using an oscillation period corresponding to the first reflection optimum ($T_{\rm osc} = 2T$).

3 Reflection of thermal atoms

In this section, we consider the use of the pulsed standing-wave mirror for the reflection of atoms from a thermal beam. The initial velocity of the atoms in the x-direction is taken to follow the Maxwell-Boltzmann distribution with an average velocity of $v_{\rm ave} = 700$ m/s. The final momentum distribution of the reflected atoms is calculated both for laser pulses with a fast turn on and turn off and with a smooth (Gaussian) temporal profile. For the atomic parameters we use the values relevant for the sodium D_2 transition.

The final momentum distribution of the reflected atoms is shown in Figure 5 for a few values of the Rabi frequency. The distributions were calculated using a laser pulse with a square-type temporal profile of 10 ns length. The vertical scale gives the fraction of atoms that end up in a given final momentum state assuming that the initial thermal atomic distribution is evenly spread out over a single period of the standing-wave pattern. The number of the reflected atoms in a realistic case can be obtained by scaling the distributions with the total number of atoms in a standing-wave period. The Rabi frequencies are chosen to give an oscillation period on the order of $2T$. For the sodium D_2 transition ($S = 25.4 a_0^2 e^2$ [38]) the corresponding intensity of the laser field varies from several tens to a few hundred $\rm MW/cm^2$. Such intensities can be reached relatively easily with commercial pulsed dye lasers. By examining the figures, one notices that the number of the reflected atoms does not change significantly in the range of the Rabi frequencies considered. For example, at an atomic beam density of $5 \times 10^{11}\,\rm atoms/cm^3$ and a cross sectional beam area of $0.01\,\rm cm^2$ the total number of the reflected atoms will be approximately 10×, 30× and $100 \times 10^3\,\rm atoms/cm$ at Rabi frequencies of 2×, 3.4× and $10 \times 10^{12}\ \rm s^{-1}$, respectively. However, since the atomic dynamics in a pulsed standing wave is strongly dependent on the ratio of the oscillation period to the interaction time, the shape of the final momentum distribution depends on the value of the Rabi frequency.

In Figure 5a, the Rabi frequency was chosen to give an oscillation period that satisfies the first reflection condition ($T_{\rm osc} \approx 2T$). For elastic reflection, the final momentum distribution should then start from zero and increase in value for the more negative momentum states. Since the reflection by a pulsed standing-wave mirror includes an anharmonic contribution, the final momentum distribution in Figure 5a contains some inelastically reflected atoms even at the optimum choice of the parameter values. In particular, the contribution of these inelastically reflected atoms is observed in the low momentum states whose occupation would otherwise be very small. Also, since the depth of the effective potential is limited, the momentum of the reflected atoms cannot exceed $m v_{\rm max}/\hbar k_\Lambda$. This corresponds to the most negative occupied momentum state of the distribution in Figure 5a.

The distributions in Figures 5b and 5c have been calculated for Rabi frequencies that correspond to a non-optimum value of the oscillation period. In Figure 5b, the Rabi frequency was chosen such that the reflected atoms would be more evenly distributed in the momentum space. If the effective potential was purely harmonic, the final momentum of the atoms would depend only on the initial

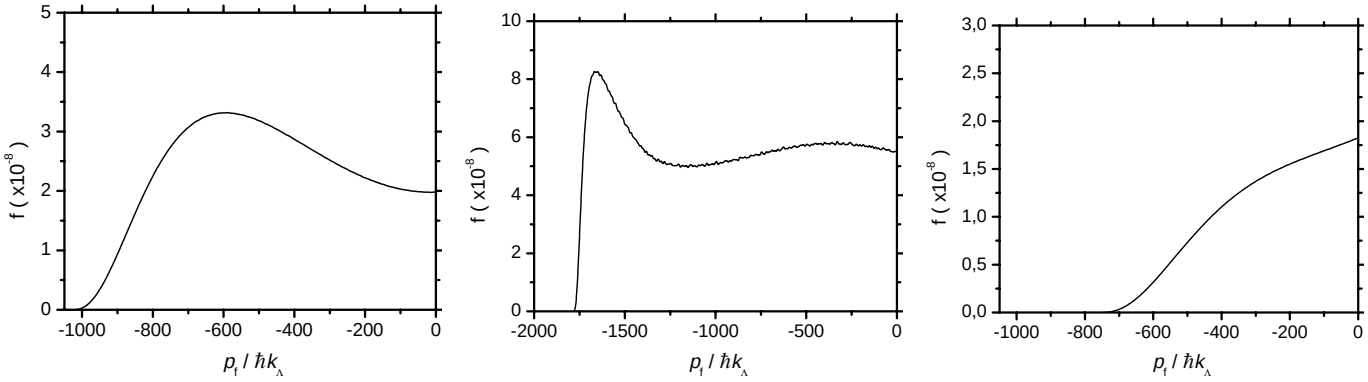

Fig. 5. The final momentum distribution of a thermal beam of sodium atoms after interaction with a pulsed standing wave. The distributions are calculated using laser pulses with a fast turn on/off and a duration of 10 ns. The initial atomic distribution is chosen to be evenly distributed over the interaction region formed by one period of the standing-wave pattern. For (a) $\Omega_0 = 3.4 \times 10^{12}$ s^{-1} and $\Delta = 1.7 \times 10^{13}$ s^{-1} ($T_{\rm osc} \approx 19$ ns), (b) $\Omega_0 = 1 \times 10^{13}$ s^{-1} and $\Delta = 5 \times 10^{13}$ s^{-1} ($T_{\rm osc} \approx 11$ ns), and (c) $\Omega_0 = 2 \times 10^{12}$ s^{-1} and $\Delta = 1 \times 10^{13}$ s^{-1} ($T_{\rm osc} \approx 25$ ns). The wavelength of the laser field is 589 nm and the angle between the laser beams is 180 degrees, in all cases. The vertical axis gives the fraction of atoms of the initial thermal distribution that end up in a final momentum state $m\hbar k_\Lambda$, where m is an integer.

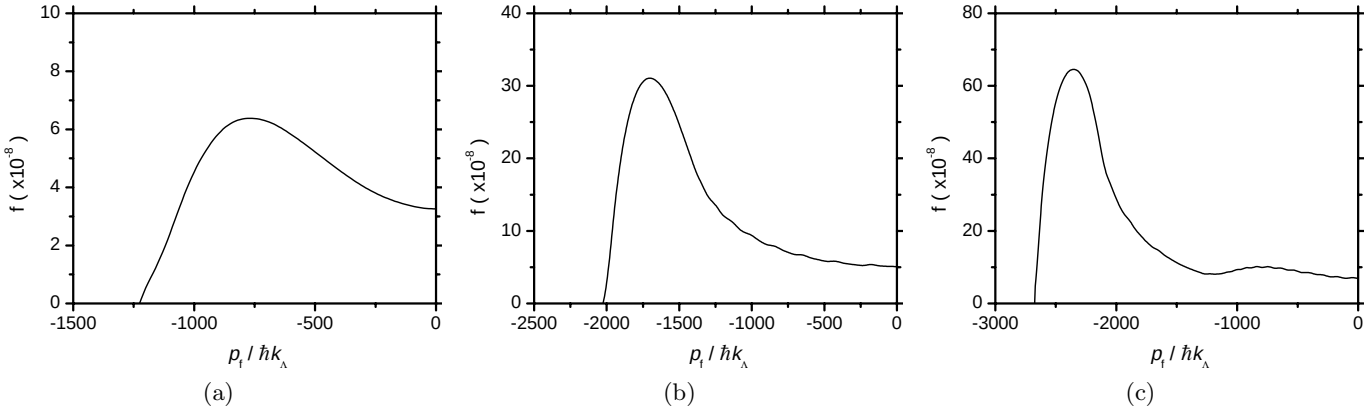

Fig. 6. The final momentum distribution of a thermal beam of sodium atoms after interaction with a pulsed standing wave. The distributions are calculated using laser pulses with a Gaussian temporal profile. The e^{-2} width of the Gaussian profile is 10 ns. The initial atomic distribution is chosen to be evenly distributed over the interaction region formed by one period of the standing-wave pattern. For (a) $\Omega_0 = 7.7 \times 10^{12}$ s^{-1} and $\Delta = 3.8 \times 10^{13}$ s^{-1}, (b) $\Omega_0 = 2.4 \times 10^{13}$ s^{-1} and $\Delta = 1.2 \times 10^{14}$ s^{-1}, and (c) $\Omega_0 = 4.6 \times 10^{13}$ s^{-1} and $\Delta = 2.3 \times 10^{14}$ s^{-1}. The wavelength of the laser field is 589 nm and the angle between the laser beams is 180 degrees, in all cases. The vertical axis gives the fraction of atoms of the initial thermal distribution that end up in a final momentum state $m\hbar k_\Lambda$, where m is an integer.

x-coordinate value of the atomic position for oscillation periods satisfying $T_{\rm osc} = 2T/(n - 1/2)$. For this case, the reflected atoms would be evenly distributed in momentum states ranging from $-mv_{\rm max}$ to 0. Although the reflection by a pulsed standing-wave mirror is not purely harmonic, a fairly even final momentum distribution of atoms is possible, as indicated by Figure 5b ($T_{\rm osc} \approx 4T/3$). Finally, in Figure 5c we show that with a suitable choice of the Rabi frequency it is possible to reflect the atoms in such a way that the occupation is highest around zero momentum.

Figure 6 shows the final momentum distribution of the reflected atoms when using a laser pulse with a Gaussian temporal profile given by

$$I_0(t) = I_0 \exp(-8t^2/T^2). \quad (9)$$

In this case, T is the e^{-2} width of the pulse and I_0 is the amplitude of the intensity modulation of the standing-wave pattern. The pulse area for the given profile is about 11% smaller than the area of a square pulse of the same peak intensity. In Figure 6a, I_0 was chosen such that the fraction of the elastically reflected atoms is optimized ($T_{\rm osc} \approx 2T$). In this case, the temporal profile of the pulse does not have a significant effect on the reflection dynamics and the final momentum distribution turns out to be

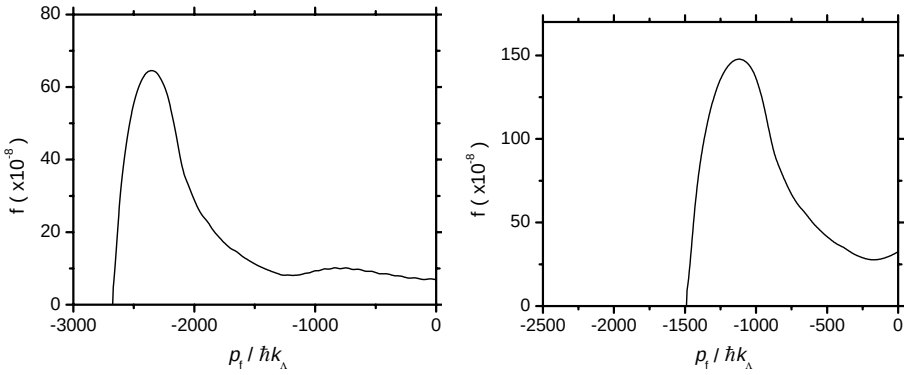

Fig. 7. The final momentum distribution of a thermal beam of sodium atoms after interaction with a moving standing wave. The distributions are calculated using laser pulses with a Gaussian temporal profile. The e^{-2} width of the Gaussian profile is 10 ns. The intensity of the laser pulse corresponds to a Rabi frequency of $\Omega_0 = 4.6 \times 10^{13}$ s^{-1} ($\Delta = 2.3 \times 10^{14}$ s^{-1}), *i.e.*, to the second reflection optimum. In (a) $v_{\rm sw} = 0$ m/s and (b) in $v_{\rm sw} = 35$ m/s. The wavelength of the laser field is 589 nm and the angle between the laser beams is 180 degrees. The vertical axis gives the fraction of the atoms of the initial thermal distribution that end up in a final momentum state $m\hbar k_\Lambda$, where m is an integer.

similar to that in Figure 5a. The main difference is that the first reflection optimum occurs at a slightly higher peak intensity than was found in the case of a square-profile laser pulse. At higher intensities ($T_{\rm osc} < T$), the pulse profile will have a more significant influence on the shape of the final momentum distributions. In Figure 6b, I_0 was increased to give $T_{\rm osc} \approx T$. In this case, the slow atoms that move in the most harmonic part of the effective potential are transmitted and thus the low negative momentum states are only slightly populated. However, the standing wave can still reflect certain anharmonically moving atoms which have a suitable initial velocity. These atoms form the population concentration in the high negative momentum states of the final momentum distribution shown in Figure 6b. Figure 6c corresponds to the second reflection optimum ($T_{\rm osc} \approx 2T/3$) for the harmonically moving atoms. In this case, the shape of the final momentum distribution at low momentum states is again similar to that of Figure 5a and the anharmonically reflected atoms have moved to higher negative momentum states. At still higher intensities, the distribution acquires more maxima which correspond to atoms that start at different reflected initial velocity groups. Since the maxima are located at high momentum states, we conclude that the shape of the final momentum distribution is more difficult to control when using a smooth laser pulse than was found for the case of square-profile pulses.

The control on the final momentum distribution can be improved by using the moving standing wave introduced in Section 2. In this case, the atoms are reflected with respect to the momentum state $mv_{\rm sw}/\hbar k_\Lambda$. Therefore, by changing the velocity of the standing-wave pattern the final momentum of the reflected atoms can be chosen appropriately. In Figure 7 we compare the final momentum distribution of the reflected atoms for the cases of a stationary and a moving standing-wave pattern ($v_{\rm sw} = 35$ m/s). The field intensity was chosen to give $T_{\rm osc} \approx 2T/3$ for the harmonically moving atoms ($n = 2$). It is seen that the position of the maximum occupation of the momentum states can be changed by varying the standing-wave velocity. In particular, with a suitable choice of the standing-wave velocity the occupation maximum can be moved to zero momentum. Thus, the moving standing wave can be used to generate slow atoms even when using smooth laser pulses. The scheme of the moving standing wave might, therefore, be interesting, for example, for generation of slow atoms in cases where the normal laser cooling methods are inefficient. This could include multilevel atoms or at somewhat higher intensities even molecules. By applying a few moving standing-wave pulses in succession it might also be possible to transfer fast atoms or molecules to low momentum states even at moderate laser intensities.

4 Summary

Reflection of neutral atoms by a pulsed standing wave with a duration in the nanosecond range was studied. The effects of the laser field on the atomic motion were described by the effective potential resulting from the adiabatic atom-photon interaction at large detunings. The equations of motion for the atomic center of mass were solved in the quasiclassical limit and the momentum distribution of the atoms was determined after interaction with a single laser pulse. The results show, that with a proper choice of the field intensity and pulse duration each period of the standing-wave pattern functions as an independent mirror for atoms with initial kinetic energy lower than the depth of the effective potential. When using a laser pulse with a fast turn on and turn off, the fraction of the elastically reflected atoms was found to be more than 20% for the first reflection optimum. This result will not change considerably when using a more realistic pulse

shape such as, *e.g.*, a laser beam with a Gaussian temporal profile. However, at higher laser intensities ($T_{\rm osc} < T$) the pulse profile can have a significant influence on the reflection dynamics. For example, a pulsed standing wave with a square-type temporal profile reflects most efficiently atoms that start close to the antinodes of the standing wave (red detuning). In contrast, when using a laser pulse with a smooth temporal profile, the standing wave reflects most efficiently atoms in certain initial velocity groups. To optimize the fraction of the elastically reflected atoms, the period of the standing-wave pattern should be chosen such that $T_{\rm osc} \approx 2T$.

The pulsed standing-wave mirror offers a few important advantages as compared with the conventional atom mirrors. The node separation of a standing-wave pattern is typically less than $1\,\mu$m. Thus, an interaction region between the laser field and an atomic beam can readily contain tens of thousands of the atom mirrors. Each of them will provide the same dipole force to the atoms and act in concert to allow manipulation of a large volume of neutral atoms simultaneously with a single laser pulse. In addition, when using pulsed lasers as the light source the depth of the effective potential is high enough to allow reflection of an order of magnitude faster atoms as compared with an atom mirror realized using a CW laser. This together with the large interaction volume should make the pulsed standing-wave mirror valuable for applications requring both strong interaction and insensitivity to the details of the internal energy level structure of the particles. The possible applications might include, for example, large angle reflection of atomic beams and even reflection of thermal atoms at normal incidence. We show that with a moderately intense laser beam (several tens of MW/cm^2) tens of thousands of atoms can be reflected from a thermal atomic beam by the mirror. Furthermore, the momentum distribution of the reflected atoms can be modified by changing the field intensity, the pulse duration or the period of the standing-wave pattern, while not significantly affecting the number of the reflected atoms.

As a further improvement on the pulsed standing-wave mirror, we propose to use a small frequency difference between the two counter-propagating laser beams to form a moving standing-wave pattern. In this case, atoms are reflected with respect to the atomic momentum that corresponds to the velocity of the standing-wave pattern. Therefore, with a proper choice of the standing-wave velocity, the energy that can be transferred to the atoms approaches in magnitude the depth of the modulation of the effective potential regardless of the initial velocity of the atoms. This offers a possibility to use a pulsed standing wave to manipulate atomic motion at high initial velocities. For example, by using a few moving standing-wave pulses in succession, it might be possible to transfer atoms with a velocity of a few hundreds of meters per second to low final momentum states even with moderately intense laser pulses. At higher intensities and by using far-off resonant interaction, this might even be a viable method to slow down multilevel atoms and even molecules, for which the conventional atom optical components are ineffective.

We gratefully acknowledge financial support from the Academy of Finland and from the national Finnish graduate school of modern optics and photonics. The computing facilities of CSC were essential for the numerical work. PR gratefully acknowledges a grant from the Jenny and Antti Wihuri Fund.

References

1. A.P. Kazantsev, G.I. Surdutovish, V.P. Yakovlev, *Mechanical Action of Light on Atoms* (World Scientific, Singapore, 1990).
2. C.S. Adams, M. Sigel, J. Mlynek, Phys. Rep. **240**, 143 (1994).
3. *Atom Interferometry*, edited by P. Berman (Academic Press, San Diego, 1997).
4. R.J. Cook, R.K. Hill, Opt. Commun. **43**, 258 (1982).
5. V.I. Balykin, V.S. Letokhov, Yu.B. Ovchinnikov, A.I. Sidorov, JETP Lett. **45**, 353 (1987).
6. M.A. Kasevich, D.S. Weiss, S. Chu, Opt. Lett. **15**, 607 (1990).
7. Yu.B. Ovchinnikov, I. Manek, R. Grimm, Phys. Rev. Lett. **79**, 2225 (1997).
8. L. Santos, L. Roso, Phys. Rev. A **58**, 2407 (1998).
9. N. Friedman, R. Ozeri, N. Davidson, J. Opt. Soc. Am. B **15**, 1749 (1998).
10. See also V.S. Letokhov, V.G. Minogin, Appl. Phys. **17**, 99 (1978).
11. C.G. Aminoff, A.M. Steane, P. Bouyer, P. Desbiolles, J. Dalibard, C. Cohen-Tannoudji, Phys. Rev. Lett. **71**, 3083 (1993).
12. M.A. Ol'Shanii, Yu.B. Ovchinnikov, V.S. Letokhov, Opt. Commun. **98**, 77 (1993).
13. M.J. Renn, D. Montgomery, O. Vdovin, D.Z. Anderson, C.E. Wieman, E.A. Cornell, Phys. Rev. Lett. **75**, 3253 (1995).
14. P. Szriftgiser, D. Guéry-Odelin, M. Arndt, J. Dalibard, Phys. Rev. Lett. **77**, 4 (1996).
15. L. Cognet, V. Savalli, G.Zs.K. Horvath, D. Holleville, R. Marani, N. Westbrook, C.I. Westbrook, A. Aspect, Phys. Rev. Lett. **81**, 5044 (1998).
16. S. Feron, J. Reinhardt, S. Le Boiteux, O. Gorceix, J. Baudon, M. Ducloy, J. Robert, Ch. Miniatura, S. Nic Chormaic, H. Haberland, V. Lorent, Opt. Commun. **102**, 83 (1993).
17. T. Esslinger, M. Weidenmuler, A. Hemmerrich, T.W. Hänsch, Opt. Lett. **18**, 450 (1993).
18. W. Seifert, C.S. Adurns, V.I. Balykin, C. Heine, Y. Ovchinnikov, J. Mlynek, Phys. Rev. A **49**, 3814 (1994).
19. R. Kaiser, Y. Levy, N. Vansteenkiste, A. Aspect, W. Seifert, D. Leipold, J. Mlynek, Opt. Commun. **104**, 234 (1994).
20. V.S. Voĭtsekhovich, M.V. Danileĭko, A.M. Negriĭko, V.I. Romanenko, L.P. Yatsenko, JETP Lett. **59**, 408 (1994).
21. H. Stapelfeldt, H. Sakai, E. Constant, P.B. Corkum, Phys. Rev. Lett. **79**, 2787 (1997).
22. A. Goepfert, I. Bloch, D. Haubrich, F. Lison, R. Schütze, R. Wynands, D. Meschede, Phys. Rev. A, R3354 (1997).
23. H. Sakai, A. Tarasevitch, J. Danilov, H. Stapelfeldt, R.W. Yip, C. Ellert, E. Constant, P.B. Corkum, Phys. Rev. A **57**, 2794 (1998).
24. V.A. Grinchuk, A.P. Kazantsev, E.F. Kuzin, M.L. Nagaeva, G.A. Ryabenko, G.I. Surdutovich, V.P. Yakovlev, JETP Lett. **34**, 375 (1981).

25. V.A. Grinchuk, E.F. Kuzin, M.I. Nagaeva, G.A. Ryabenko, V.P. Yakovlev, JETP Lett. **57**, 549 (1993).
26. P. Ryytty, M. Kaivola, C.G. Aminoff, Quant. Semiclass. Opt. **10**, 545 (1998).
27. P. Ryytty, M. Kaivola, C.G. Aminoff, Eur. Phys. J. D **7**, 369 (1999).
28. J. Dalibard, C. Cohen-Tannoudji, J. Opt. Soc. Am. B **2**, 1707 (1985).
29. C. Cohen-Tannoudji, J. Dupont-Roc, G. Grynberg, *Atom-Photon Interactions* (John Wiley & sons, New York, 1992).
30. M.D. Crisp, Phys. Rev. A **8**, 2128 (1973).
31. E. Wigner, Phys. Rev. **40**, 749 (1932).
32. R. Cook, Phys. Rev. A **22**, 1078 (1980).
33. E. Arimondo, A. Bambini, S. Stenholm, Phys. Rev. A **24**, 898 (1981).
34. A.P. Kazantsev, G.A Ryabenko, G.I. Surdutovich, V.P. Yakovlev, Phys. Rep. **129**, 77 (1985).
35. Similar results can be obtained also for the atomic deflection by a standing wave, *cf.*, A.F. Bernhardt, B.W. Shore, Phys. Rev. A **23**, 1290 (1981); E. Arimondo, A. Bambini, S. Stenholm, Opt. Commun. **37**, 103 (1981); C. Tanguy, S. Reynaud, M. Matsuoka, C. Cohen-Tannoudji, Opt. Commun **44**, 249 (1983); Yu.B. Ovchinnikov, J.H. Müller, M.R. Doery, E.J.D. Vredenbregt, K. Helmerson, S.L. Rolston, W.D. Phillips, Phys. Rev. Lett. **83**, 284 (1999).
36. M.K. Olsen, T. Wong, S.M. Tan, D.F. Walls, Phys. Rev. A **53**, 3358 (1996).
37. The tendency of the pulsed standing wave to reflect atoms that start at certain initial velocity groups, when using laser pulses with a smooth temporal profile, leads to a similar bifurcated final momentum distribution as a function of initial velocity as is observed for atoms crossing a CW standing wave with a Gaussian spatial profile, see Q. Li, G.H. Baldwin, H.-A. Bachor, D.E. McClelland, J. Opt. Soc. Am. B **13**, 257 (1996).
38. W.L. Wiese, M.W. Smith, B.M. Glennon, National Standard Reference Data Series, Vol. 22 (U.S. Government Printing Office, Washington D.C., 1969).